Why we need better outcome metrics for VHL: RECIST may be just one data point.

Does the solid component of CNS hemangioblastoma progress on belzutifan — or are we measuring it the wrong way?
One patient, eight lesions, two verdicts

The Hemangioblastoma Research Project

A program of the Rath Family Foundation · rathfoundation.org

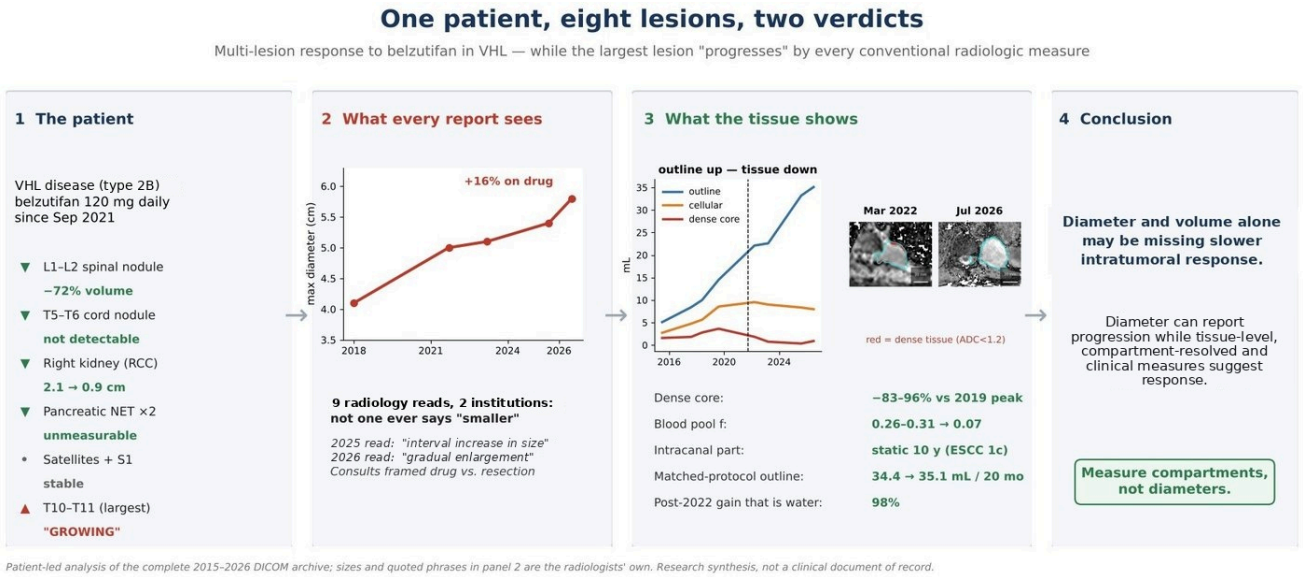
Updated 2 November 2026. Supersedes the patient-led preprint draft of 14 October 2026; text matches the web version at rathfoundation.org/case-study.

Abstract

Five lesions responded in ways no one disputes, and two millimeter-scale sentinels never changed. The eighth — the largest — was called "growing" on every conventional read for five years, while the tissue inside it may tell a different story.

Patient TR is an adult male with von Hippel–Lindau disease (type 2B) and roughly three decades of multisystem disease. He has taken the HIF-2α inhibitor belzutifan, 120 mg daily, since September 2021. His complete 2015–2026 imaging archive was re-measured voxel by voxel. RECIST — the Response Evaluation Criteria in Solid Tumors — and the size-based criteria like it were built to judge cytotoxic chemotherapy in malignant tumors: shrinkage is response, growth is failure. This case shows how that ruler may come up short in hemangioblastoma — a contradiction between what the radiology record says about his largest lesion and what the lesion's interior is doing, on a drug whose earliest effects are vascular rather than cell-killing.

Presented as a patient-led analysis of a complete 2015–2026 imaging archive (233,014 DICOM images), prepared with large-language-model assistance and primary-source verification, shared with the patient's permission. This is a research synthesis, not a clinical document of record; nothing here is a treatment recommendation.



The whole case on one panel. The patient and his eight lesions; what every radiology report sees in the index lesion; what the tissue-level measurements show inside it; and the question it raises — whether RECIST-style size criteria, built for cytotoxic chemotherapy, can report progression in a lesion whose tissue measures may be responding to an anti-vascular drug.

1 The patient and the eight lesions

Three tumor types, three organ systems, one outlier by the ruler

Within six months of starting belzutifan, each of the five larger non-index lesions in Patient TR's body lost more than half its volume; the millimeter-scale satellites and the right S1 root lesion, below reliable volumetry, were unchanged. Systemic drug effect is not in question: his hemoglobin

Table 1. Lesion-by-lesion response summary. The shrinkers were not growing before treatment; the index lesion was doubling every ~2.8 years and was 15–140× larger than any other lesion, so size and prior growth cannot be separated with one outlier. The ranking (pancreatic > renal > CNS hemangioblastoma) matches the trials.[14,40]

Lesion	Pre-treatment (2015–2021)	On belzutifan	Mid-2026
L1–L2 intradural nodule conus tip, among cauda equina	6.0–6.6 mm, no growth	3.7 mm at 6 mo (38% of baseline volume); 23% at 17 mo; 28% at 4 y	2–4 mm dot, still enhances; best in-CNS sentinel
T5–T6 cord-surface nodule + cord edema	~3 × 5 mm, no growth; edema 6–17 mm	Edema absent from the day-5 scan onward (scanner-era caveat); nodule ~halved by Mar 2022; feeder vessel gone by Aug 2023	No measurable nodule — cleanest complete response
Right kidney mass ccRCC per reports; prior cryoablation ×2, partial nephrectomy	2.1 × 1.8 cm, "unchanged" vs 2018–2019 (report, Sep 2021)	"Decreased in size from prior," 1.6 × 1.2 cm at 6 mo (report, Mar 2022); −78% self-derived volume at 17 mo, flat after	0.9 cm, "no diffusion restricted nodularity" (report, Aug 2025); no identifiable enhancing tissue
Pancreatic NET, upper head	1.1 × 0.8 cm, "unchanged" vs 2018 (report, Sep 2021)	"Smaller and less conspicuous," 0.7 × 0.6 cm at 6 mo; "no longer discretely measurable" by Feb 2023	"Not distinctly seen" (report, Aug 2025)
Pancreatic NET, uncinate	12–16 mm (2018–19); 7 mm by Sep 2021 on somatostatin analog	Not measurable on treatment	Not judgeable
Millimeter-scale spinal satellites; right S1 root lesion	Unchanged	Unchanged and enhancing	Tracked as sentinels
T10–T11 index lesion left extradural paravertebral dumbbell, solid, never cystic	Growing, doubling ~2.8 y; 24.5 mL at drug start (first full-coverage MRI)	Every clinical read reported growth; tissue metrics regressed (section 3)	~35 mL protocol-locked / ~43–44 mL hi-res full coverage; pain improved; cord unchanged (ESCC 1c stable)

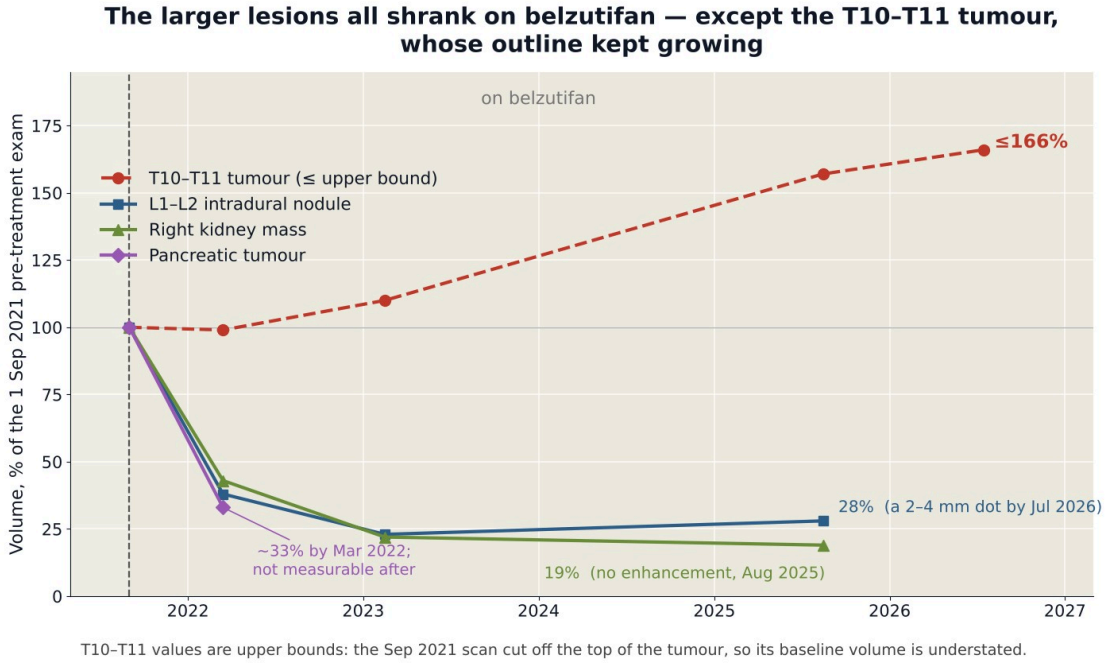


Figure 1 · The measurable lesions on one chart. Each line is one lesion's volume as a percentage of the 1 September 2021 pre-treatment exam. Every plotted lesion except the T10–T11 line drops by more than half within ~6 months and stays down; the millimeter-scale sentinels, unchanged throughout, sit below reliable volumetry and are not plotted. The T10–T11 line is an upper bound because its baseline scan cut off the top of the lesion.

has sat at the low plateau that erythropoietin suppression produces for five years (9.9 g/dL, August 2025), and the responding lesions' regression is radiologist-documented at both treating institutions.

Pre-treatment history relevant here: prior somatostatin-analog therapy 2019–2021 and long-standing off-label propranolol, with quantitatively limited effect on the index lesion.[39] The 1 September 2021 abdominal MRI is the true pre-treatment baseline; the 14 September 2021 spine MRI is approximately day 5 on drug. The lesion-by-lesion record is below. Sizes and quoted phrases in the table are the radiologists' own; volume percentages are from this analysis.

2 What every report sees

Nine reads, five years on treatment, never once "smaller"

The index lesion is a left T10–T11 extradural "dumbbell" hemangioblastoma at the nerve root — epidural and paravertebral components through the left neural foramen, abutting but not compressing the cord (ESCC 1c — epidural spinal cord compression grade 1c, dural contact without

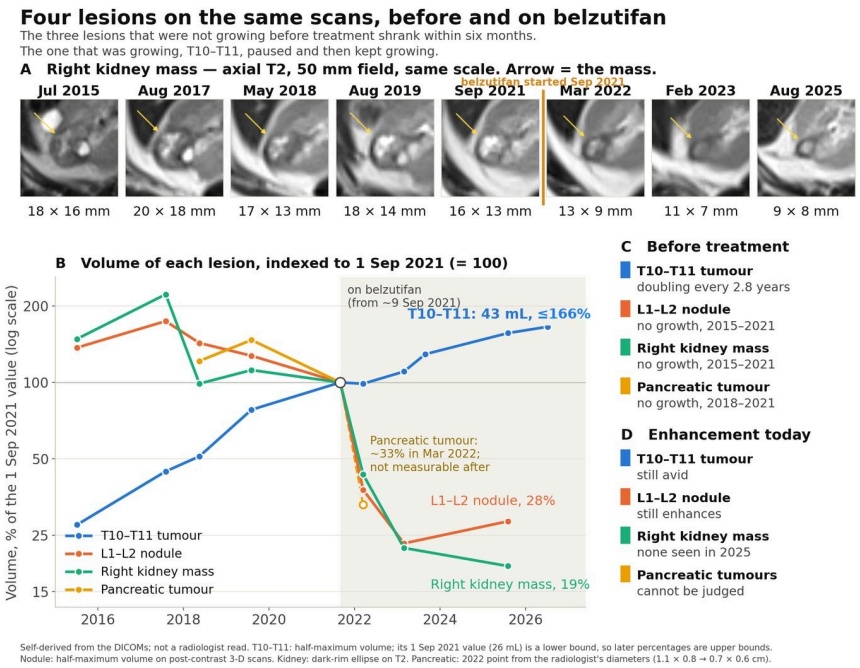


Figure 2 · Four lesions, same scans, same timeline. Top: the right-kidney mass on matched axial T2 windows, 2015⟶2025 — visibly stable before treatment, then shrinking (18 × 16 ⟶ 9 × 8 mm; the radiologists' reads: 2.1 × 1.8 ⟶ 1.6 × 1.2 ⟶ 0.9 cm). Bottom: each lesion's volume indexed to the September 2021 baseline (= 100). The kidney, L1–L2 nodule and pancreatic lesion fall together in the first six months; only the T10–T11 outline rises.

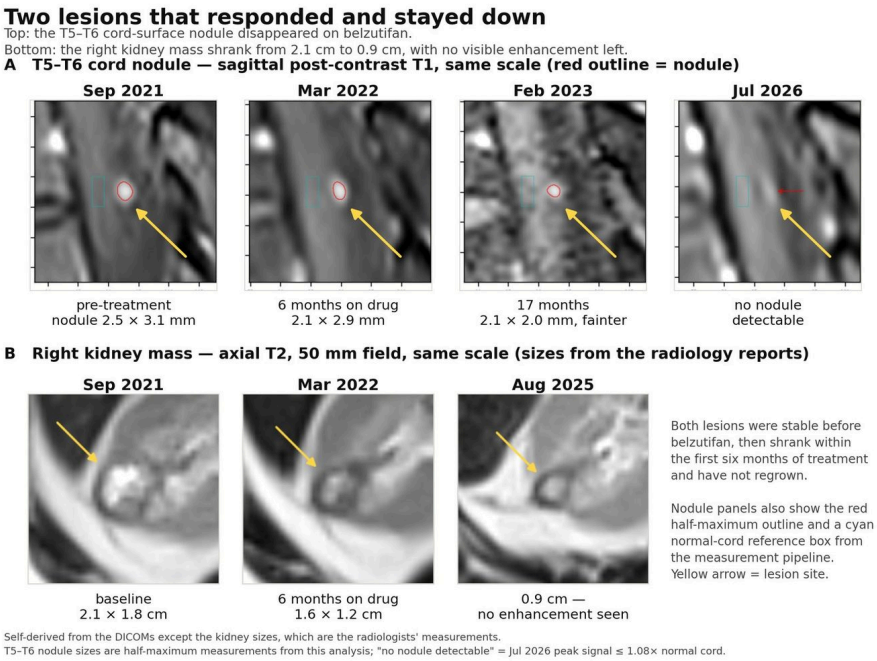


Figure 4 · Two radiologist-tracked responders. Top: the T5–T6 cord-surface nodule from pre-treatment through July 2026, when its peak signal is no longer separable from normal cord (≤ 1.08×). Bottom: the right kidney mass with the radiologists' own measurements — 2.1 × 1.8 cm at baseline, "decreased in size" to 1.6 × 1.2 cm at six months, 0.9 cm with no visible enhancement by August 2025.

cord deformity — on every exam 2016–2026), solid throughout, with no associated cyst or peritumoral edema on any exam from 2015 to 2026. The institutional record for it, verbatim, is below.

The stakes were not hypothetical. Roughly six months after belzutifan initiation, a senior neurosurgeon at one institution read the first on-treatment MRI as growth and recommended resection. The other institution's report on that same March 2022 exam read the lesion as "essentially stable in size," and the voxel-level measurements below place the lesion's cellular peak and turn in that same month. The clinical record over the same interval moved the other way: radicular pain in the left rib and abdomen present before the first dose had "subsided within the last few months" by May 2022; the April

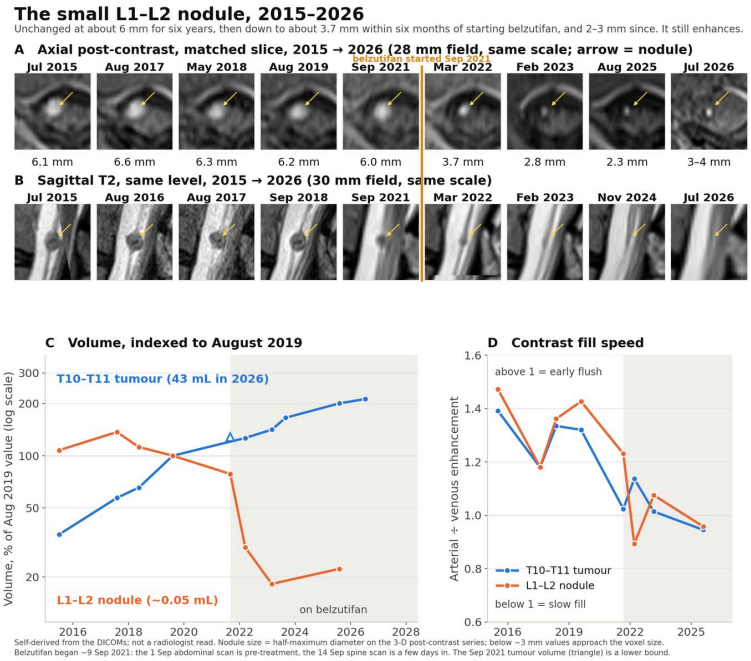


Figure 3 · The in-canal sentinel. The L1–L2 intradural nodule, 2015–2026: matched post-contrast slices each year show the nodule shrinking from 6.1 mm to a 2–4 mm dot (6.1 ⟶ 3.7 ⟶ 2.8 ⟶ 2.3 mm). This is what response looks like when a hemangioblastoma is small and unencapsulated.

Table 2. The institutional radiology record for the index lesion, 2018–2026, from two institutions' reports (retrieved October 2026). The 14 September 2021 exam is ~day 5 on belzutifan and is effectively the pre-treatment spine baseline. No report in the series ever describes the lesion as smaller.

Exam date	Reported T10–T11 size (radiologist)	Impression wording (verbatim)
2018 (reference)	4.1 × 2.7 × 1.6 cm (spine read); 3.7 × 2.5 cm lateral (abdominal read)	—
Sep 1, 2021	4.9 × 3.3 cm (lateral)	"…has mildly increased in size"
Sep 14, 2021 (day ~5)	5.0 × 3.2 × 2.9 cm (addendum)	"…appears increase since 2018… Mass effect at the T10 canal appears slightly increased"
Mar 16, 2022	4.8 × 3.2 × 3.1 cm (spine); 4.5 × 3.4 cm lateral (abdomen)	"…essentially stable in size"; other hemangioblastomas "stable or slightly decreased"; renal mass "decreased in size from prior"
Feb 28, 2023	5.1 × 3.7 × 3.4 cm	"Mild interval enlargement… Stable mild mass effect upon the T10-T11 cord"
Aug 29, 2023	5.2 × 3.7 × 3.4 cm	"…stable in appearance"
Apr 16, 2024	4.0 × 4.9 cm	"Stable exam"
Nov 7, 2024	— ("stable… unchanged")	"Stable exam since April 16, 2024"
Aug 6, 2025	5.4 × 4.0 cm	"Interval increase in size of left thoracic paraspinal mass"
Jul 10, 2026	5.8 × 4.6 cm	"Gradual enlargement of the enhancing mass… Unchanged mass effect on the thecal sac without progressive cord compression or cord edema"

2023 neurosurgical note records improvement of lower back pain, a fully normal examination, and a patient who "runs 5–10 miles without issues." No clinician currently recommends intervention on the index lesion. The neurosurgical consultations have nonetheless been framed as a choice between staying on the drug and resecting — the framing this analysis is meant to inform.

3 What the tissue shows

Inside the "growing" lesion, the cellular compartment peaked at month six and regressed

Before treatment (2015–2019), total volume, integrated cellular mass and dense cellular core tripled in lockstep — what genuine growth looks like. On treatment they split: the outline kept rising while every tissue-level measure turned down.

The central divergence

Integrated cellular mass peaked at 9.54 mL in March 2022 and declined to 7.96 mL by July 2026 (−17% on two-compartment diffusion mixing; −33% if the shrinking microvascular blood pool is subtracted first). The dense cellular core collapsed from its 2019 peak of 3.63 mL to 0.15–0.61 mL (−83% to −96%), reproducing the ~84% median solid-component regression of

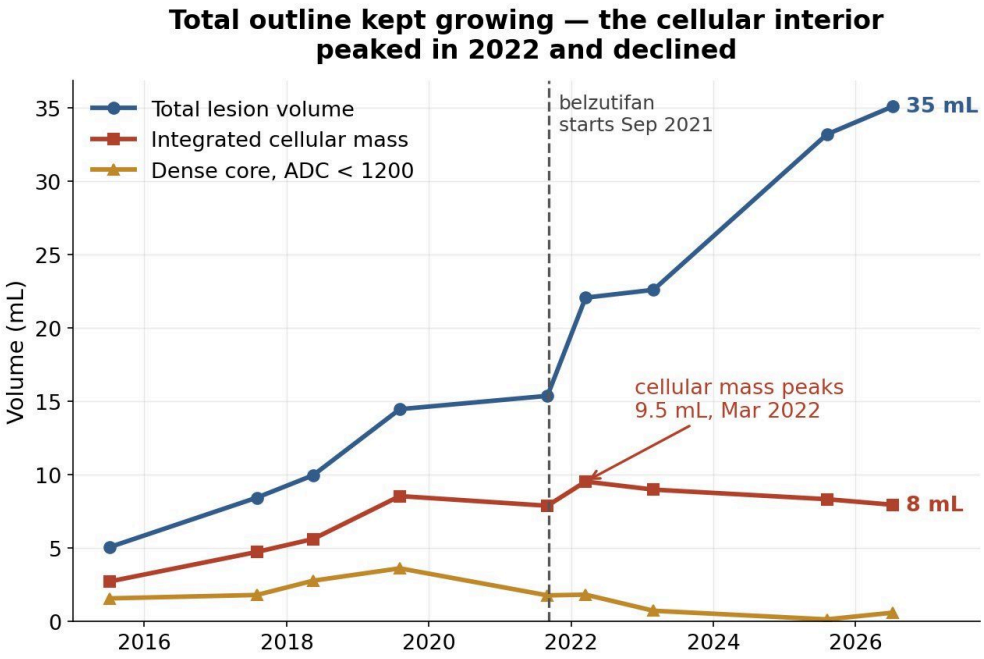


Figure 5a · The central divergence. Blue: total outline volume (what the ruler sees). Orange: integrated cellular mass. Red: dense core. Before belzutifan all three rise together — real growth. On treatment the blue line keeps climbing while the tissue lines peak in March 2022 and fall.

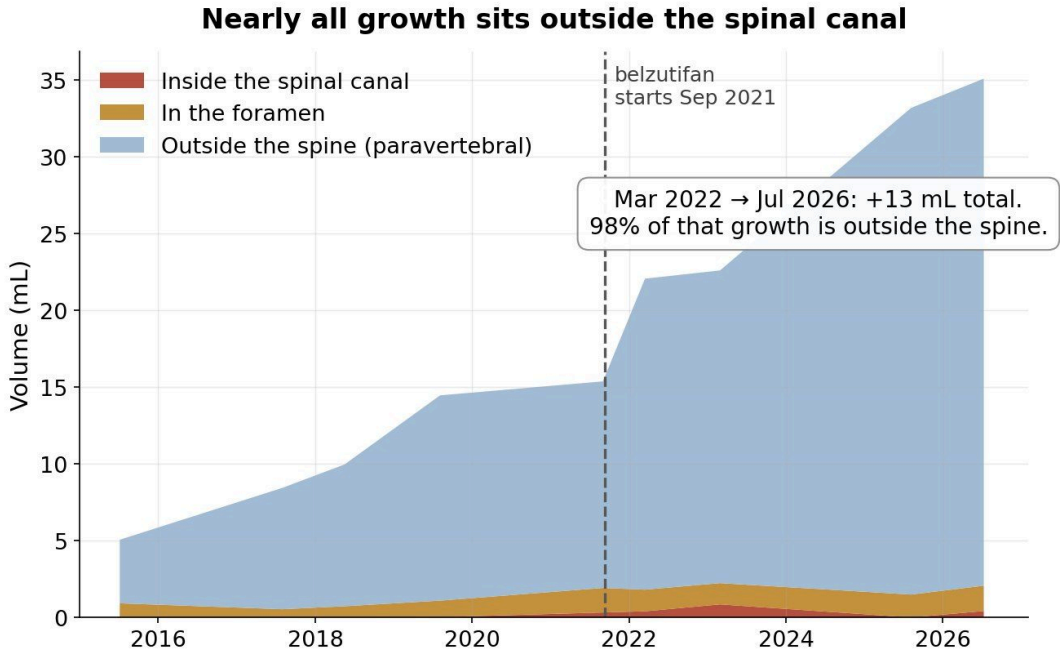


Figure 5b · Where the added volume went. Volume stacked by anatomic zone: 98% of the post-2022 gain is in the unconfined extradural space; the slice inside the spinal canal is static.

trial responders.[15] The dense core's share of the total outline fell from 31% (2015) and 25% (2019) to 0.5–3.3% (2023–2026); every ADC percentile rose monotonically. Meanwhile 98% of the post-2022 volume gain accrued in the unconfined extradural (paravertebral) space; the component inside the spinal canal has been static for ten years (+0.02 mL), with ESCC 1c unchanged on every exam.

The dense core and the resistant-clone check

Three-dimensional connected-component analysis of dense voxels answers the resistant-clone question directly: the only contiguous ADC < 1.2 component ≥ 1 mL existed in March 2022 (1.64 mL) and collapsed to ~0.24 mL, flat since (2023: 0.29; 2025: 0.24; 2026: 0.24 mL largest). No contiguous dense focus ≥ 1 mL has existed since March 2022. A resistant subclone would appear here first — as one growing piece, not scattered rim flecks.

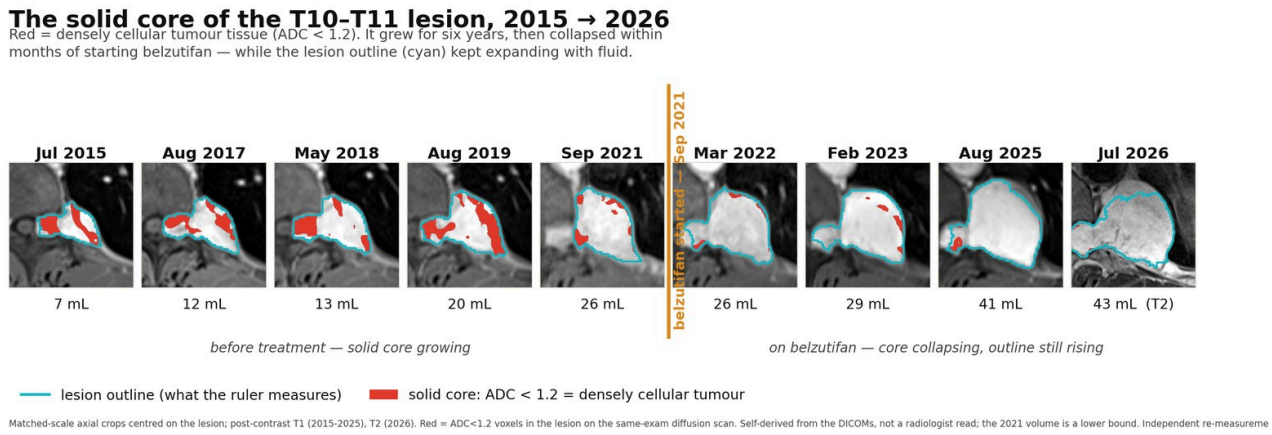


Figure 6c · The solid core, 2015 ⟶ 2026, on the actual images. Matched-scale axial crops centered on the lesion across eleven years. Red marks the densely cellular core (ADC < 1.2 × 10^{-3} mm²/s) inside the cyan outline. Before belzutifan (amber line, September 2021) the red core grows with the lesion; within months of starting the drug it collapses and keeps shrinking, while the outline the ruler measures keeps expanding with fluid. Post-contrast T1 2015–2025, T2 for 2026.

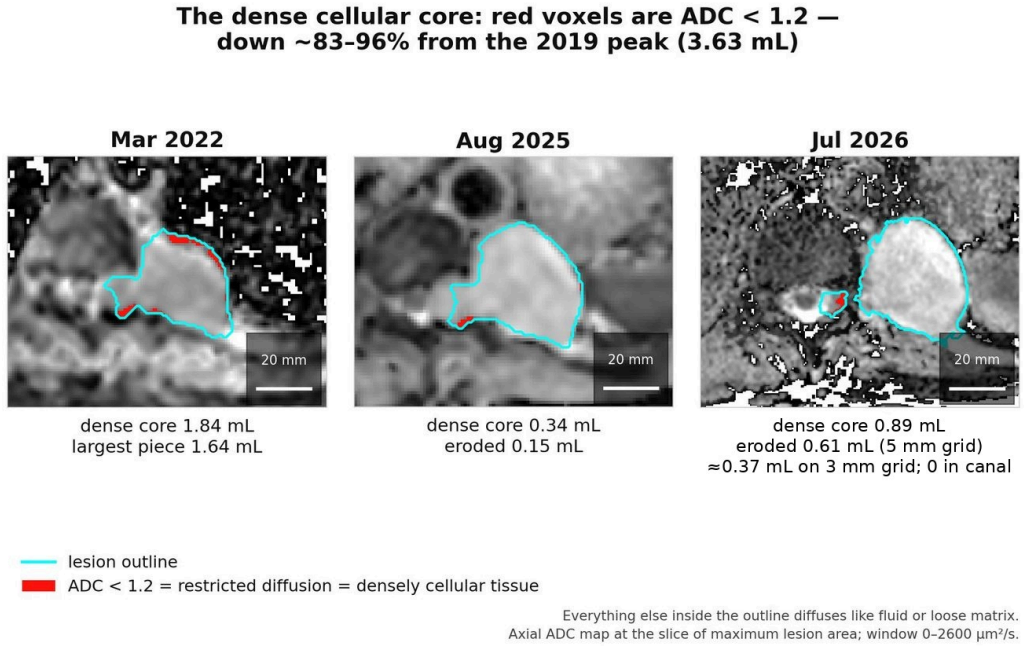


Figure 7 · How the dense-core collapse is measured, on the actual images. Each panel is the axial ADC map at the slice of maximum lesion area; cyan is the lesion outline; red marks every voxel with ADC < 1.2 × 10^{-3} mm²/s — the diffusion signature of densely cellular tissue. In March 2022 the red already hugs the margin instead of forming an interior core; by 2025–2026 the interior is uniformly water-like and the remaining red is boundary flecks (these flecks are boundary pixels shared with pedicle bone; stripping one pixel from the edge of the mask — the "eroded" values — removes them). Against the 2019 peak of 3.63 mL, the dense core is down ~83–96%.

Water content and vascular physiology

The ADC distribution of the whole lesion shifted toward free water: the median rose from 1362 (2019) to 2062 × 10^{-6} mm²/s (July 2026), and even the densest decile now sits above the dense-tissue cutoff. Within each comparable diffusion family the IVIM microvascular perfusion fraction collapsed (f ≈ 0.26–0.31 ⟶ 0.07–0.08), and contrast kinetics inverted from arterial flush-and-washout (2015–2019 arterial/venous/delayed relative enhancement ≈ 313/241/211%) to slow progressive accumulation (2025: 333/387/384%, delayed ≥ arterial). Intralesional T2 flow-void voxels fell to zero by 2024. The dominant feeder's caliber persisted and arterial inflow did not fall — the lesion is not devascularized; rather, the immature VEGF-dependent exchange bed and its washout physiology have regressed, which is what HIF-2α/VEGF withdrawal should produce.[13,28,41] The radiology record carries independent corroboration: the March 2022 spine read noted the T5–T6 lesion's "prominent feeding vessels… are less prominent."

De-confounding the ruler: the protocol-locked series

The decisive de-confounding comes from holding the protocol fixed. On the longitudinally consistent 5 mm axial T2 sequence, whole-lesion volume was 34.4 mL on 7 November

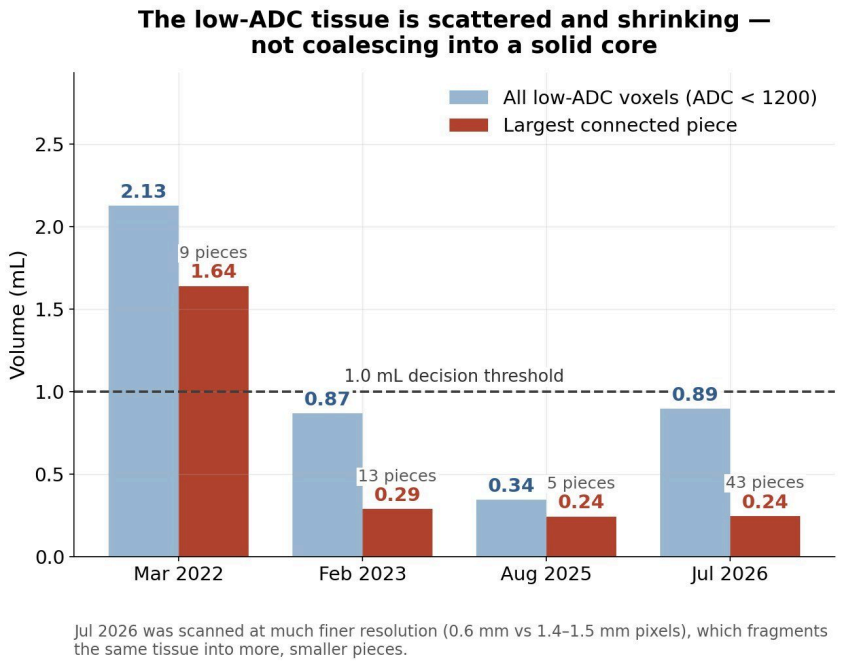


Figure 8 · The resistant-clone check. For each study, the total dense volume and the single largest contiguous dense piece, against the 1.0 mL decision threshold: no contiguous dense focus ≥ 1 mL has existed since March 2022, and the largest piece has been flat at ~0.24 mL for four years.

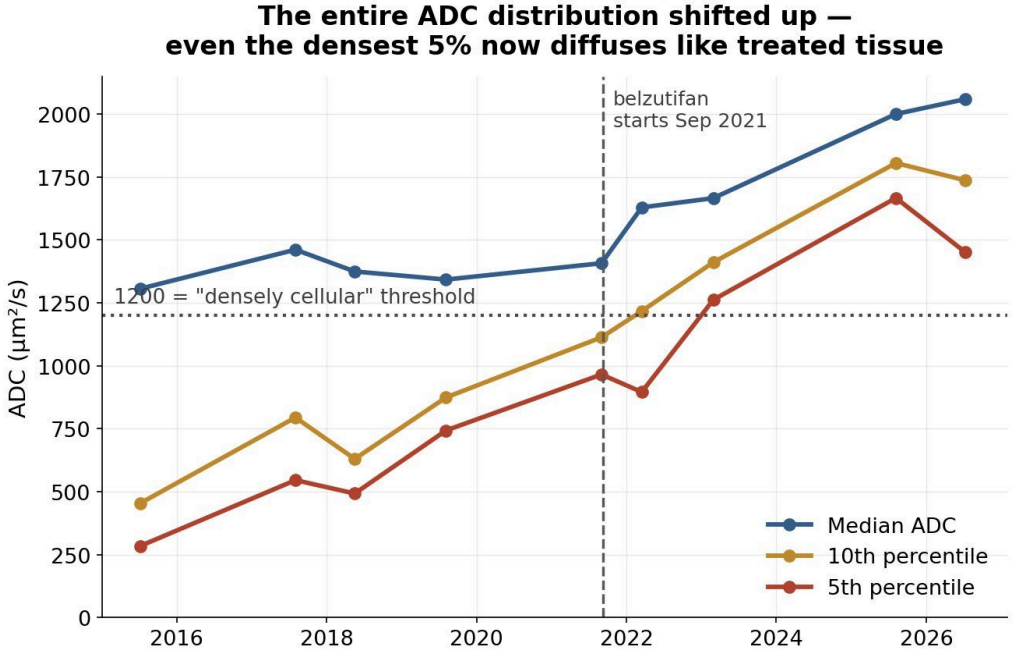


Figure 6a · ADC percentiles over time. ADC measures how freely water diffuses: low = dense cellular tissue, high = fluid. The lesion's percentiles rise year over year — even its densest decile (p10) now sits above the dense-tissue cutoff (1200, dashed).

2024 and 35.1 mL on 10 July 2026 — a 20-month change of +0.7 mL (≈ +1%/yr; the extraspinal component −0.1%/yr). The widely quoted 43–44 mL figure for July 2026 comes from a same-day 3 mm high-resolution sequence that covers ~51 mm of craniocaudal extent versus ~31 mm routine and segments at a lower effective threshold. Wider coverage and the looser threshold each contribute to the same-day +9.0 mL difference: the ruler changed, not the lesion. A second convention — segmenting at half the lesion's maximum signal — still gives ~6%/yr in the last interval. Read together, the honest statement is deceleration to at-or-near plateau on like-for-like measurement, a sharp break from the pre-treatment ~29%/yr.

Robustness: under loose, middle and tight masks alike, cellular mass peaks in March 2022 and declines (10.43⟶8.59 / 9.54⟶7.96 / 8.74⟶7.27 mL) and the dense core collapses 75–96% from the 2019 peak. Across a 16-combination grid of assumed diffusivities, 12 show declining cellular mass from

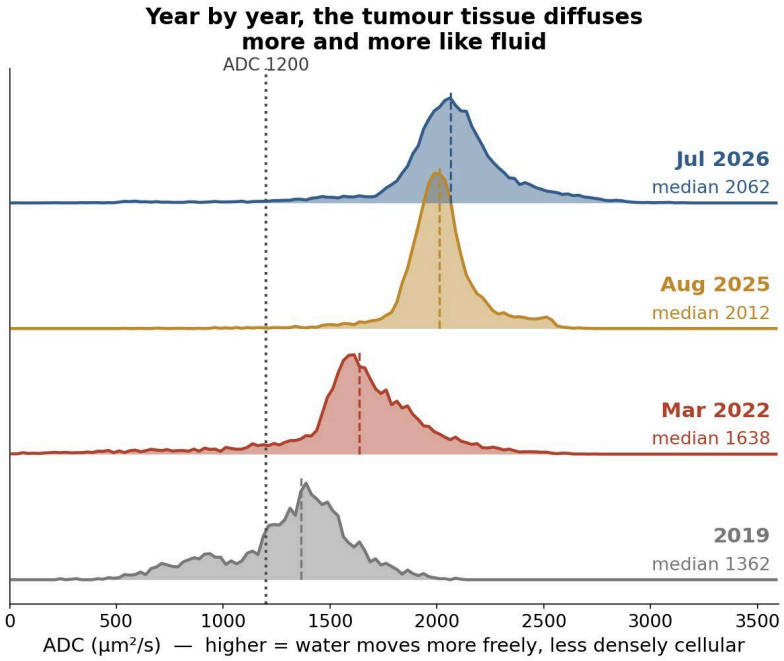


Figure 6b · The whole ADC distribution. Four representative years — the entire lesion marches toward free-water diffusivity.

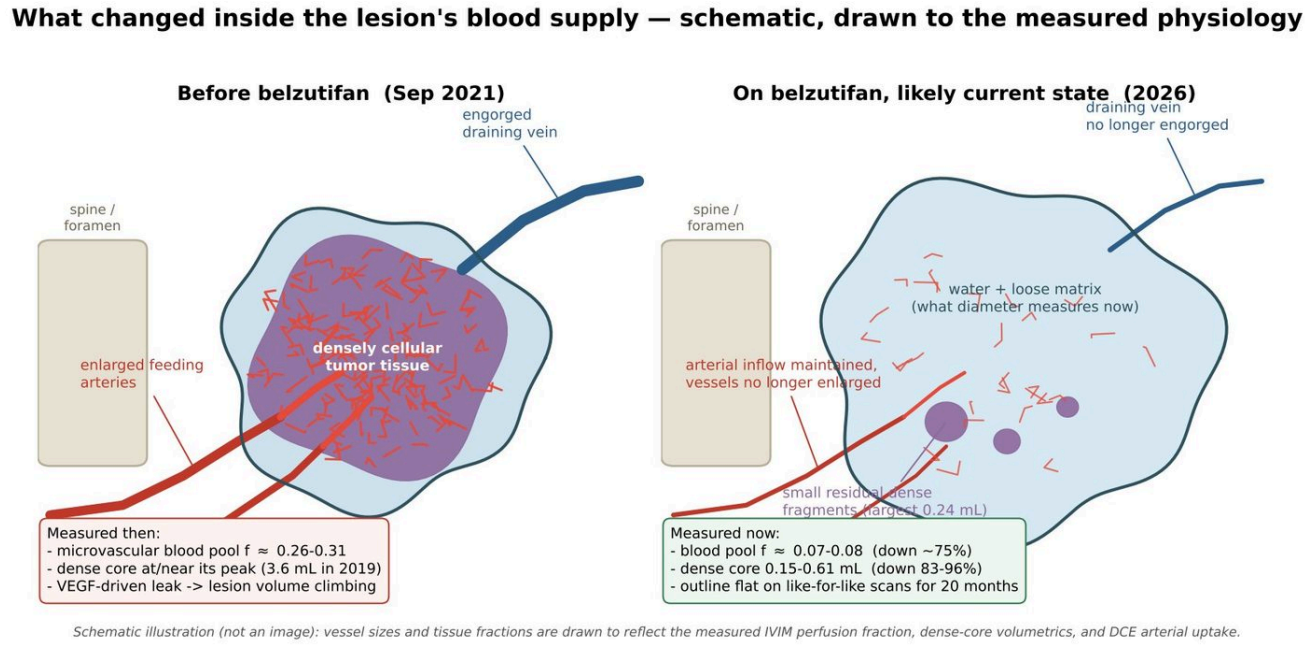


Figure 10 · Before and on drug, schematically. Drawn to the measured quantities, not traced from an image. Before (left): enlarged feeders, a dense immature VEGF-dependent capillary bed (IVIM perfusion fraction f ≈ 0.26–0.31), an engorged draining vein, and a predominantly cellular interior. Now (right): arterial inflow persists but the exchange bed has involuted (f ≈ 0.07–0.08), the dense tissue has collapsed to small fragments (largest 0.24 mL), and the outline — unchanged for 20 months on like-for-like scans — encloses mostly water and loose matrix, which is what the diameter measurements track.

the March 2022 baseline; only free-water-at-body-temperature ceilings produce growth. Cross-scanner harmonization against same-scan paraspinal muscle preserves the trend across four scanners and eleven years. The claim robust to every plausible assumption is no material cellular growth over five years on treatment; the decline is the likely, constants-dependent reading.

4 Where RECIST and other chemotherapy-era criteria may fall short here

Measurement convention, as much as biology, shapes the verdict

RECIST was built for cytotoxic chemotherapy in malignant tumors: response = shrinkage (≥30% in summed diameters), progression = ≥20% growth. Three properties of this setting

Table 3. The index lesion by the ruler versus by the tissue (middle mask; ADC in 10^{-6} mm²/s; cellular mass and dense core from the diffusion-capable studies). Bold volumes are the like-for-like protocol pair: 34.4 ⟶ 35.1 mL in 20 months. * Sep 2021 abdominal study truncated the lesion top: values are lower bounds. † Measured on a finer 0.6 mm grid whose boundary partial-volume voxels against pedicle bone inflate the raw value; one-voxel erosion on the 5 mm mask gives 0.61 mL, and the 3 mm high-resolution mask gives ≈0.37 mL with 0.00 mL in the canal and foramen. ‡ The same-session high-resolution series covers ~51 mm craniocaudal versus ~31 mm routine and segments at a lower effective threshold (tumor/muscle ratio 2.98 ⟶ 7.20) — the ruler changed, not the lesion.

Date	Series family	Total outline (mL)	Cellular mass (mL)	Dense core ADC < 1.2 (mL)	ADC p10
2015-07	abdominal 3-D T1	5.1	2.73	1.58	454
2017-08	abdominal	8.4	4.75	1.81	795
2018-05	abdominal	10.0	5.63	2.79	630
2019-08	abdominal	14.5	8.55	3.63 — peak	874
2021-09-01 *	abdominal (truncated)	15.4*	7.89*	1.79*	1113
2021-09-14	spine T2 (day ~5)	24.5	—	—	—
2022-03	abdominal / spine T2	22.1 / 20.2	9.54 — peak	1.84	1218
2023-02	abdominal / spine T2	22.6 / 26.8	8.99	0.74	1411
2023-08	spine T2	33.4	—	—	—
2024-11	spine T2	**34.4**	—	—	—
2025-08	abdominal	33.2	8.34	0.34 (0.15 eroded)	1805
2026-07	spine T2 (matched 5 mm)	**35.1**	7.96	0.89 † (0.61 eroded)	1737 (1804 eroded)
2026-07	spine T2 3 mm hi-res	44.1 ‡	—	≈0.37 (0.8%; 0.00 canal/ foramen)	1861

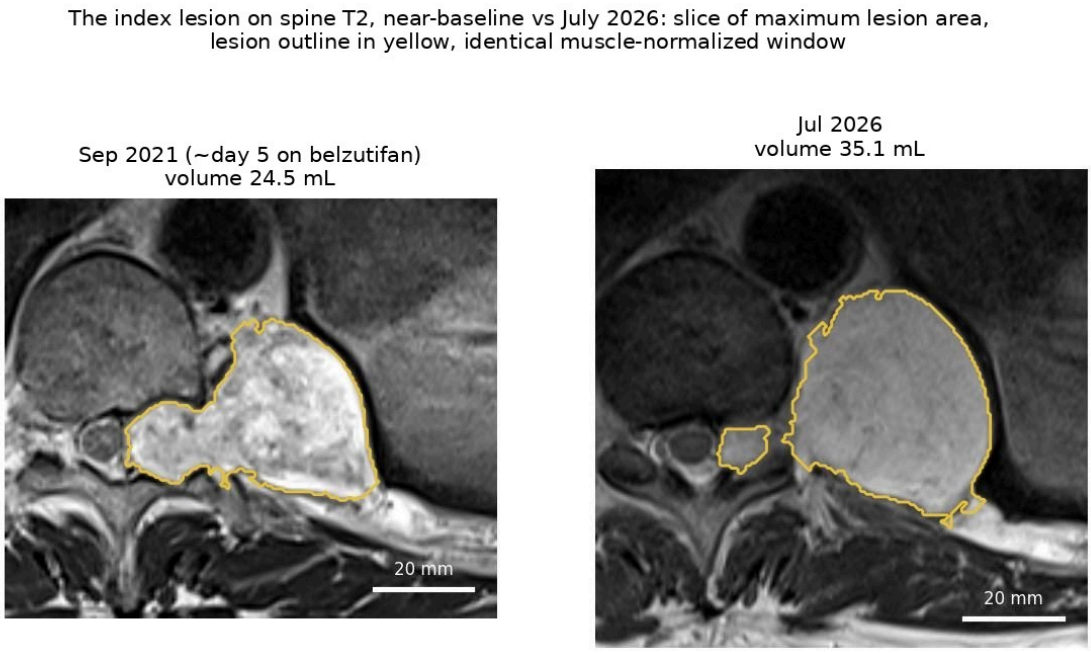


Figure 9 · Independent cross-check on a different sequence family. The same lesion on spine T2, near-baseline (14 September 2021, ~day 5 on drug) versus July 2026, windows normalized to same-scan muscle: the 2026 lesion is larger but brighter-fluid in signal character — more water signal, not more tissue signal.

strain those assumptions, and this case displays all three at once.

The drug's primary effect is vascular The earliest true responses are de-permeabilization phenomena — edema off, leak off, perfusion down — that no diameter captures.[41]

The measured compartment determines the verdict In the registration study's own CNS data, cyst-inclusive reading gives a 44% objective response rate where solid-only reading of the same patients gives 76%.[15]

Fluid can replace tissue inside a fixed boundary Size can rise while tumor regresses — this lesion's exact behavior, inside a fibrous extradural boundary tethered to

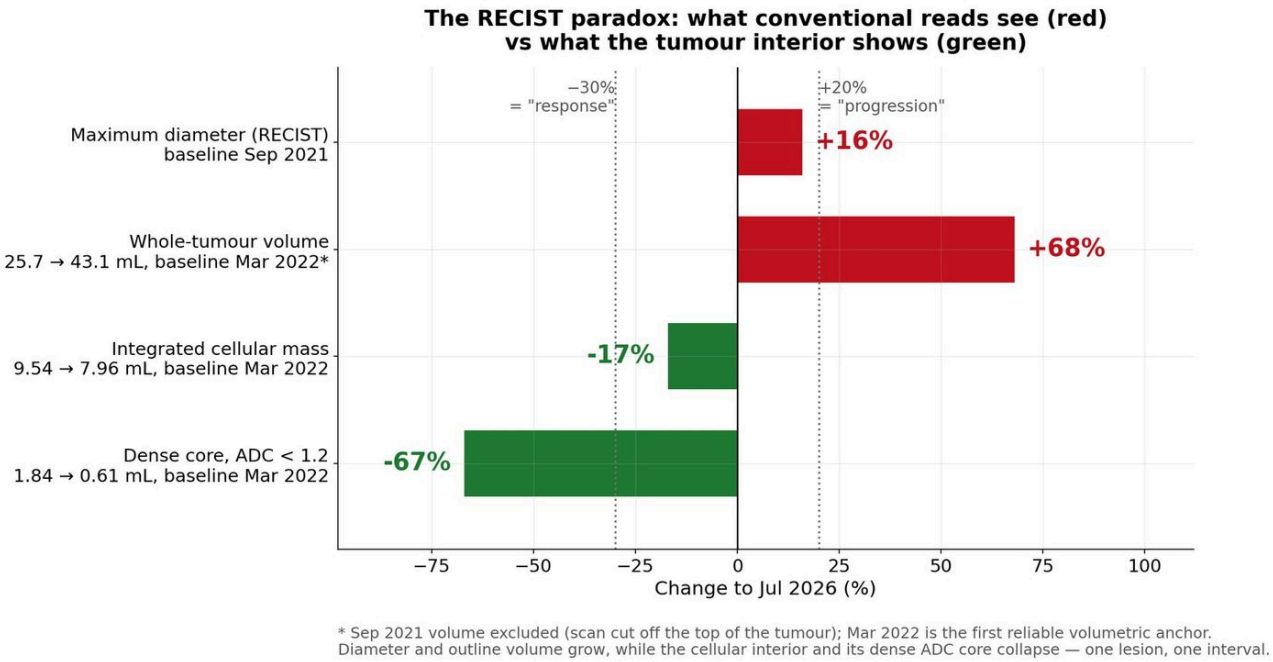


Figure 11 · Four readings of the same lesion over the same treatment interval. Red bars are what conventional assessment sees: maximum diameter +16% (vs the September 2021 baseline; "stable disease" against the RECIST ±20/−30% reference lines) and half-maximum volume +68% (March 2022 anchor). Green bars are what the tissue shows over the same interval: integrated cellular mass −17%, dense core −67% (1.84 ⟶ 0.61 mL on the 5 mm eroded grid; ≈ −80% on the 3 mm grid; −83 to −96% against the 2019 peak). Measurement convention, as much as biology, shapes whether this lesion is called progressing, stable, or responding.

rib head, vertebral body and pleura that cannot collapse inward the way a millimeter-scale intradural nodule can.

Read this way, the case stops being anomalous. A solid, cyst-free hemangioblastoma "progressing" on belzutifan is undocumented: a structured review of the indexed literature (PubMed, October 2026) found no published report of confirmed progression of the solid component of a CNS hemangioblastoma on belzutifan. Apparent enlargement in this disease is characteristically cyst-driven — which is why the registration study scored responses both cyst-inclusive and solid-only[15] — and the one real-world series that separates target from non-target lesions states that progression occurred only as "the emergence of new lesions," with "no progression… in the primary target lesions."[43] What the measurements suggest this lesion is doing — accumulating treatment-associated fluid while its tumor tissue regresses — resembles the familiar cyst phenomenon of CNS hemangioblastoma[9,10,15] expressed interstitially, inside an encapsulated extradural boundary, rather than as a loculated cyst. The fluid simply lacks a cyst wall to make the distinction obvious on a routine read; only tissue-level measures (diffusion, perfusion, enhancement kinetics) separate the compartments.

> *No radiology report or clinician in five years has ever recorded a sign of improvement in this lesion — not a measurement artifact so much as a gap in what the standard instruments can see — a change that diffusion, perfusion and compartment analysis do register.*
>
> *— Patient-led analysis, October 2026*

The March 2022 exam captures the inversion in miniature: a single scan that one neurosurgical consultation read as growth warranting resection, the institutional radiology report read as "essentially stable," and the tissue-level measurements identify as the cellular compartment's peak and turning point. Each read was correct on its own terms. That no reader ever saw improvement is the point, not a footnote: the standard instruments appear to have little sensitivity to this drug's mechanism of action in solid tissue, which is reason to test whether size change should be the primary outcome at all.

A fourth reported quantity, which a three-compartment convention omits

The reporting standard now being proposed for this disease — report enhancing nodule, cyst and edema volumes separately rather than as one summed measurement — would be a substantial improvement. It is also, on the evidence of this lesion, incomplete in one specific way. Those are three *volumes*. A lesion that has lost its cellular fraction under HIF-2α inhibition and gained interstitial water *without* forming a cyst is scored entirely as nodule, reported as stable or slowly progressive on size, and the largest change in it does not enter the record at all. That is this case.

Median apparent diffusion coefficient within this lesion was flat at 1.37 and 1.36 ($\times 10^{-3}$ mm²/s) in 2015 and 2019 — unchanged through a threefold increase in volume — and then rose to 1.42, 1.64, 1.68, 2.01 and 2.07 at September 2021, 2022, 2023, 2025 and 2026. Over the September 2021 to February 2023 interval, on the same scanner at the same *b*-values, the rise was 18% against a skeletal-muscle reference of −2%. The

non-enhancing share *fell* over the same period, 2.8% to 0.6%: no cyst formed.

A rise in diffusivity inside a hypervascular tumor is ambiguous on its own, because blood is also mobile water, and conventional monoexponential diffusion imaging cannot separate a lesion filling with interstitial fluid from one filling with blood. Here intravoxel incoherent motion imaging separated them, and the two terms moved in opposite directions: tissue diffusivity rose from 1.0–1.2 to approximately 2.0 while the perfusion fraction collapsed from 0.26–0.31 to 0.07–0.08, which is skeletal-muscle level. **Water up, blood down.**

The suggestion this case supports is therefore a fourth reported quantity: **within the enhancing volume, tissue diffusivity reported together with perfusion fraction, against a same-exam reference tissue.** It is a qualifier on the nodule volume rather than a fourth segmentation — the compartment has no boundary to outline — and acquisition and fitting should follow the published multi-organ consensus recommendations so that results remain comparable between sites.[44] Two things make this cheaper than it sounds: diffusion sequences are already acquired in most spine and brain protocols, so for many archived studies the measurement is retrospective; and the known weakness of the technique, that protocol heterogeneity produces non-comparable parameters, now has a published remedy.

What it would buy is the distinction that volume cannot make. A lesion whose cellular fraction is falling while its volume rises may be a responding lesion filling with water. A lesion whose cellular fraction holds while its volume rises is more likely a tumor that is still growing. Those two situations call for opposite decisions, they are indistinguishable on diameter, and at present there is no prospective means of telling them apart.

Three limits should be stated with it. This is one lesion. It is extradural, where leaked plasma distributes through the tumor's own interstitium because that space has lymphatic drainage and no containing envelope; an intradural lesion, where the same leak pools against a glial wall and forms a cyst, may partition its fluid differently, so the generalization to intramedullary or posterior fossa disease is untested. And the one published intratumoral study of a HIF-2α inhibitor, in metastatic renal carcinoma, reported that diffusion imaging was not informative[28] — with the monoexponential readout that is precisely the one expected to fail in a hypervascular lesion. Whether the separated parameters behave differently in a more vascular, more stromal tumor is untested in either direction. This is offered as a hypothesis with a worked example attached, not as a validated biomarker.

5 What this means for the project

Measurement is a treatment question

A patient on the only approved drug for this disease can be steered toward spinal surgery by a measurement convention. In this case the recommendation to resect came six months into treatment, on the exam that tissue-level analysis identifies as the turning point. Decisions anchored to total size alone risk operating on water.

The project's primary outcome variable is the number of surgical procedures a person with VHL hemangioblastoma undergoes in a lifetime. Disability in this disease accrues across repeated CNS surgery,[11,12] and the strongest real-world signal for belzutifan is a fall in VHL-related procedures from 0.35 to 0.08 per patient-year, a reduction of roughly three-quarters.[18] If the instruments used to judge response cannot see response, that outcome is put at risk by the measurement itself — not by the disease or the drug.

That is why Direction 1 — three-compartment reporting, with nodule, cyst/fluid and edema measured and reported separately — and Direction 3 — a growth model that can certify a lesion safe to watch — sit first in the research agenda. Both are tractable with existing imaging; neither requires a new drug. The measurement lesson of the registration study (count the solid, not the fluid[15]) needs to be extended to encapsulated lesions that accumulate the same fluid interstitially, and mechanism-concordant markers — perfusion fraction, diffusion percentiles, enhancement kinetics, protocol-locked volumes, procedures per year, symptom burden — need to be tested as the decision variables for this drug class.

What the patient asked of the treating team

No management decisions have been made; nothing is scheduled or agreed. The central request is human, independent reanalysis, because the single largest limitation of the analysis is that it is one patient-side pipeline.

6 Limitations

What this analysis is, and is not

This is a patient-led synthesis compiled with large-language-model assistance and independent cross-review, with citations verified against PubMed; it is structured preparation for clinical judgment, not a substitute for it. All imaging analyses are self-derived with research-grade processing, not radiologist reads. Segmentations come from one analyst pipeline (three mask variants tested; no independent re-segmentation). The index-lesion record spans four scanners and multiple diffusion protocols; harmonization was checked but is imperfect. The September 2021 baseline is truncated. Cellular-mass estimates are model-dependent in absolute terms. Small-lesion measurements (1.4–6 mm on 3 mm slices) carry large relative uncertainty; pancreatic lesions are arterial-timing-dependent and their course after six months is genuinely indeterminate; the renal site carries prior ablation and surgical change. The index-lesion diagnosis is clinico-radiographic, without tissue (~85–95% confidence; an alternative differential of schwannoma was raised by the treating team in 2023). Boundary-erosion magnitudes depend on the measurement grid. The 2021 report of the patient's earlier course is a non-peer-reviewed preprint.[39]

References

1. Maher ER, Yates JR, Harries R, et al. Clinical features and natural history of von Hippel-Lindau disease. Q J Med. 1990;77(283):1151-63. PMID 2274658. doi:10.1093/qjmed/77.2.1151
2. Kaelin WG. Von Hippel-Lindau disease: insights into oxygen sensing, protein degradation, and cancer. J Clin Invest. 2022;132(18):e162480. PMID 36106637. doi:10.1172/JCI162480
3. Binderup ML, Smerdel M, Borgwadt L, et al. von Hippel-Lindau disease: updated guideline for diagnosis and surveillance. Eur J Med Genet. 2022;65(8):104538. PMID 35709961. doi:10.1016/j.ejmg.2022.104538
4. Lonser RR, Butman JA, Huntoon K, et al. Prospective natural history study of central nervous system hemangioblastomas in von Hippel-Lindau disease. J Neurosurg. 2014;120(5):1055-62. PMID 24579662. doi:10.3171/2014.1.JNS131431
5. Zhou B, Wang J, Liu S, et al. Hemangioblastoma instead of renal cell carcinoma plays a major role in the unfavorable overall survival of von Hippel-Lindau disease patients. Front Oncol. 2019;9:1037. PMID 31649892. doi:10.3389/fonc.2019.01037
6. Park DM, Zhuang Z, Chen L, et al. von Hippel-Lindau disease-associated hemangioblastomas are derived from embryologic multipotent cells. PLoS Med. 2007;4(2):e60. PMID 17298169. doi:10.1371/journal.pmed.0040060
7. Shively SB, Edwards NA, MacDonald TJ, et al. Developmentally arrested basket/stellate cells in postnatal human brain as potential tumor cells of origin for cerebellar hemangioblastoma in von Hippel-Lindau patients. J Neuropathol Exp Neurol. 2022;81(11):885-899. PMID 35980299. doi:10.1093/jnen/nlac073
8. Vortmeyer AO, Tran MG, Zeng W, et al. Evolution of VHL tumourigenesis in nerve root tissue. J Pathol. 2006;210(3):374-82. PMID 16981244. doi:10.1002/path.2062
9. Lonser RR, Vortmeyer AO, Butman JA, et al. Edema is a precursor to central nervous system peritumoral cyst formation. Ann Neurol. 2005;58(3):392-9. PMID 16130092. doi:10.1002/ana.20584
10. Huntoon K, Wu T, Elder JB, et al. Biological and clinical impact of hemangioblastoma-associated peritumoral cysts in von Hippel-Lindau disease. J Neurosurg. 2016;124(4):971-6. PMID 26517769. doi:10.3171/2015.4.JNS1533
11. Mehta GU, Asthagiri AR, Bakhtian KD, et al. Functional outcome after resection of spinal cord hemangioblastomas associated with von Hippel-Lindau disease. J Neurosurg Spine. 2010;12(3):233-42. PMID 20192620. doi:10.3171/2009.10.SPINE09592
12. Takeshima Y, Takami H, Endo T, et al. Comparison of the recurrence and surgical outcome of spinal hemangioblastoma in sporadic and von Hippel-Lindau diseases: a subanalysis of a nationwide study by the Neurospinal Society of Japan. Neurospine. 2023;20(3):756-765. PMID 37350167. doi:10.14245/ns.2346368.184
13. Xu R, Wang K, Rizzi JP, et al. 3-[(1S,2S,3R)-2,3-Difluoro-1-hydroxy-7-methylsulfonylindan-4-yl]oxy-5-fluorobenzonitrile (PT2977), a hypoxia-inducible factor 2alpha (HIF-2alpha) inhibitor for the treatment of clear cell renal cell carcinoma. J Med Chem. 2019;62(15):6876-6893. PMID 31282155. doi:10.1021/acs.jmedchem.9b00719
14. Jonasch E, Donskov F, Iliopoulos O, et al. Belzutifan for renal cell carcinoma in von Hippel-Lindau disease. N Engl J Med. 2021;385(22):2036-2046. PMID 34818478. doi:10.1056/NEJMoa2103425
15. Iliopoulos O, Iversen AB, Narayan V, et al. Belzutifan for patients with von Hippel-Lindau disease-associated CNS haemangioblastomas (LITESPARK-004): a multicentre, single-arm, phase 2 study. Lancet Oncol. 2024;25(10):1325-1336. PMID 39284337. doi:10.1016/S1470-2045(24)00389-9
16. Srinivasan R, Iliopoulos O, Beckermann KE, et al. Belzutifan for von Hippel-Lindau disease-associated renal cell carcinoma and other neoplasms (LITESPARK-004): 50 months follow-up from a single-arm, phase 2 study. Lancet Oncol. 2025;26(5):571-582. PMID 40228516. doi:10.1016/S1470-2045(25)00099-3
17. Wiley HE, Srinivasan R, Maranchie JK, et al. Oral hypoxia-inducible factor 2alpha inhibitor belzutifan in ocular von Hippel-Lindau disease: subgroup analysis of the single-arm phase 2 LITESPARK-004 study. Ophthalmology. 2024;131(11):1324-1332. PMID 38849055. doi:10.1016/j.ophtha.2024.05.024
18. Al Abbas M, Zarka J, Silva AC, et al. Clinical outcomes of HIF-2alpha inhibition in von Hippel-Lindau disease: a multicenter real-world study. Oncologist. 2026;31(10):oyag331. PMID 42610708. doi:10.1093/oncolo/oyag331
19. Dhawan A, Peereboom DM, Stevens GH. First clinical experience with belzutifan in von Hippel-Lindau disease associated CNS hemangioblastoma. CNS Oncol. 2022;11(3):CNS91. PMID 35819008. doi:10.2217/cns-2022-0008
20. Neth BJ, Webb MJ, White J, et al. Belzutifan in adults with VHL-associated central nervous system hemangioblastoma: a single-center experience. J Neurooncol. 2023;164(1):239-247. PMID 37450072. doi:10.1007/s11060-023-04395-3
21. Yeganeh KJ, Sargent E, Ahmed G, et al. Belzutifan in von Hippel-Lindau-associated hemangioblastomas: a systematic review and meta-analysis. J Neurol Surg B Skull Base. 2025;87(5):e124-e131. PMID 42626756. doi:10.1055/a-2724-4297
22. do Amaral PS, Fonseca RB, Reisen B, et al. Long-term safety and efficacy of belzutifan in von Hippel-Lindau syndrome: a VHL coordinating care center experience. J Kidney Cancer VHL. 2025;12(3):25-31. PMID 40937004. doi:10.15586/jkc.v12i3.425
23. Winer AJ, do Amaral PS, Ryan EG, et al. The safety profile of belzutifan in renal tumors: real-world data from a tertiary academic center. Oncologist. 2025;30(9):oyaf274. PMID 40920370. doi:10.1093/oncolo/oyaf274
24. Choueiri TK, Powles T, Peltola K, et al. Belzutifan versus everolimus for advanced renal-cell carcinoma. N Engl J Med. 2024;391(8):710-721. PMID 39167807. doi:10.1056/NEJMoa2313906
25. Agarwal N, Brugarolas J, Ghatalia P, et al. Randomized phase II dose comparison LITESPARK-013 study of belzutifan in patients with advanced clear cell renal cell carcinoma. Ann Oncol. 2024;35(12):1148-1156. PMID 39233312. doi:10.1016/j.annonc.2024.08.2338
26. Marathe DD, Jauslin PM, Kleijn HJ, et al. Exposure-response analyses for belzutifan to inform dosing considerations and labeling. J Clin Pharmacol. 2024;64(10):1246-1258. PMID 38752556. doi:10.1002/jcph.2459
27. Marathe DD, Jauslin PM, Kleijn HJ, et al. Population pharmacokinetic analyses for belzutifan to inform dosing considerations and labeling. CPT Pharmacometrics Syst Pharmacol. 2023;12(10):1499-1510. PMID 37596839. doi:10.1002/psp4.13028
28. Courtney KD, Ma Y, Diaz de Leon A, et al. HIF-2 complex dissociation, target inhibition, and acquired resistance with PT2385, a first-in-class HIF-2 inhibitor, in patients with clear cell renal cell carcinoma. Clin Cancer Res. 2020;26(4):793-803. PMID 31727677. doi:10.1158/1078-0432.CCR-19-1459
29. Choueiri TK, Merchan J, Patnaik A, et al. Casdatifan shows durable response linked to HIF-2alpha biology in kidney cancer. Nature. 2026;656(8128):734-741. PMID 42386974. doi:10.1038/s41586-026-10718-x
30. Visweswaran V, Pavithran K. Belzutifan: a narrative drug review. Curr Drug Res Rev. 2022;14(2):88-95. PMID 35366789. doi:10.2174/2589977514666220401094724
31. Perona-Moratalla AB, Carrion B, Villar Gomez de Las Heras K, et al. Dual inhibition of HIF-1alpha and HIF-2alpha as a promising treatment for VHL-associated hemangioblastomas: a pilot study using patient-derived primary cell cultures. Biomedicines. 2025;13(5):1234. PMID 40427061. doi:10.3390/biomedicines13051234
32. Feldman MJ, Sizdahkhani S, Edwards NA, et al. Loss of quiescence in von Hippel-Lindau hemangioblastomas is associated with erythropoietin signaling. Sci Rep. 2016;6:35486. PMID 27748427. doi:10.1038/srep35486
33. Thomas GV, Tran C, Mellinghoff IK, et al. Hypoxia-inducible factor determines sensitivity to inhibitors of mTOR in kidney cancer. Nat Med. 2006;12(1):122-7. PMID 16341243. doi:10.1038/nm1337

34. Chittiboina P, Mandal D, Bugarini A, et al. Proteostasis modulation in germline missense von Hippel-Lindau disease. Clin Cancer Res. 2023;29(12):2199-2209. PMID 37018064. doi:10.1158/1078-0432.CCR-22-3651
35. Ahmad S, Muhlebner A, Snijders TJ, et al. Somatostatin receptor 2A expression in von Hippel-Lindau-related hemangioblastomas. Cancer. 2024;130(20):3473-3479. PMID 38824656. doi:10.1002/cncr.35418
36. Soukup J, Novakova M, Hojny J, et al. Unusual immunohistochemical profiles in hemangioblastomas and their relevance in differential diagnosis: a comprehensive study of 112 cases. J Neuropathol Exp Neurol. 2026;85(9):992-1003. PMID 41762700. doi:10.1093/jnen/nlag012
37. Jonasch E, McCutcheon IE, Gombos DS, et al. Pazopanib in patients with von Hippel-Lindau disease: a single-arm, single-centre, phase 2 trial. Lancet Oncol. 2018;19(10):1351-1359. PMID 30236511. doi:10.1016/S1470-2045(18)30487-X
38. Jonasch E, McCutcheon IE, Waguespack SG, et al. Pilot trial of sunitinib therapy in patients with von Hippel-Lindau disease. Ann Oncol. 2011;22(12):2661-2666. PMID 22105611. doi:10.1093/annonc/mdr011
39. Single-patient report describing propranolol followed by lanreotide for a VHL-associated thoracic hemangioblastoma prior to belzutifan. Research Square preprint, 2021 (PPR300322). Preprint; not peer-reviewed; not indexed in PubMed.
40. Halperin R, Tirosh A. Non-interventional management of advanced pancreatic neuroendocrine neoplasms in patients with von Hippel-Lindau disease. Cancers (Basel). 2023;15(6):1739. PMID 36980625. doi:10.3390/cancers15061739
41. Pagliara A, De Giuseppe S, Di Profio S, et al. Very rapid response to belzutifan of VHL-related intracranial and retinal hemangioblastomas. Am J Ophthalmol Case Rep. 2026;42:102565. PMID 41908298. doi:10.1016/j.ajoc.2026.102565
42. Meiman D, Skaar TC, Shugg T, Quinney SK. Physiologically based pharmacokinetic model to assess the drug-drug-gene interaction potential of belzutifan in combination with cyclin-dependent kinase 4/6 inhibitors. JCO Precis Oncol. 2025;9:e2500153. PMID 40712111. doi:10.1200/PO-25-00153
43. Rhein K, Kotsis F, Ganner A, et al. Belzutifan for patients with von Hippel-Lindau (VHL) disease-associated heterogeneous tumors — a retrospective single center analysis. BMC Cancer. 2025;25(1):1686. PMID 41174705. doi:10.1186/s12885-025-15192-8 — "Tumor progression was noted in two patients, involving the emergence of new lesions, but no progression occurred in the primary target lesions."
44. Sigmund EE, Rauh SS, Iima M, et al. Towards clinical translation of intravoxel incoherent motion MRI: acquisition and analysis consensus recommendations. J Magn Reson Imaging. 2026;63(6):1782-801. PMID 41853873. doi:10.1002/jmri.70278